HHS Public Access

Author manuscript

*Kidney Int*. Author manuscript; available in PMC 2015 September 01.

Published in final edited form as:

*Kidney Int*. 2015 March ; 87(3): 543–556. doi:10.1038/ki.2014.302.

# Phosphorylation of ribosomal protein S6 mediates compensatory renal hypertrophy

**Jinxian Xu**[1], **Jianchun Chen**[2], **Zheng Dong**[1,3], **Oded Meyuhas**[4], and **Jian-Kang Chen**[1,5,*]

[1]Department of Cellular Biology and Anatomy, Medical College of Georgia, Georgia Regents University, Augusta, Georgia, USA

[2]Division of Nephrology and Hypertension, Department of Medicine, Vanderbilt University School of Medicine, Nashville, Tennessee, USA

[3]Research Department, Charlie Norwood VA Medical Center, Augusta, Georgia, USA

[4]Department of Biochemistry and Molecular Biology, Institute for Medical Research Israel – Canada, Hebrew University-Hadassah Medical School, Jerusalem 91120, Israel

[5]Department of Medicine, Medical College of Georgia, Georgia Regents University, Augusta, Georgia, USA

## Abstract

The molecular mechanism underlying renal hypertrophy and progressive nephron damage remains poorly understood. Here we generated congenic ribosomal protein S6 (rpS6) knockin mice expressing non-phosphorylatable rpS6 and found that uninephrectomy-induced renal hypertrophy was significantly blunted in these knockin mice. Uninephrectomy-induced increases in cyclin D1 and decreases in cyclin E in the remaining kidney were attenuated in the knockin mice compared to their wild-type littermates. Uninephrectomy induced rpS6 phosphorylation in the wild type mice; however, no rpS6 phosphorylation was detected in uninephrectomized or sham-operated knockin mice. Nonetheless, uninephrectomy stimulated comparable 4E-BP1 phosphorylation in both knockin and wild type mice, indicating that mTORC1 was still activated in the knockin mice. Moreover, the mTORC1 inhibitor rapamycin prevented both rpS6 and 4E-BP1 phosphorylation, significantly blunted uninephrectomy-induced renal hypertrophy in wild type mice, but did not prevent residual renal hypertrophy despite inhibiting 4E-BP1 phosphorylation in uninephrectomized knockin mice. Thus, both genetic and pharmacological approaches unequivocally demonstrate that phosphorylated rpS6 is a downstream effector of the mTORC1-S6K1 signaling pathway mediating renal hypertrophy. Hence, rpS6 phosphorylation facilitates the increase in cyclin D1 and decrease in cyclin E1 that underlie the hypertrophic nature of uninephrectomy-induced kidney growth.



*Corresponding author: Jian-Kang Chen, Department of Cellular Biology and Anatomy, Department of Medicine, Medical College of Georgia, Georgia Regents University, 1459 Laney Walker Boulevard, Augusta, Georgia 30912, USA, Tel: 706-721-8424, Fax: 706-721-7661, jchen@gru.edu.

**DISCLOSURES**

All the authors declared no competing interests.

Supplementary informations are available in *Kidney International's* website.

**Keywords**

compensatory renal hypertrophy; uninephrectomy; mTORC1-S6K1 signaling; ribosomal protein rpS6 phosphorylation-deficient knockin mice; rapamycin

## INTRODUCTION

Reduction in the number of functioning nephrons stimulates increased protein synthesis causing increases in cell size, with minimal cell proliferation, in the components (particularly the proximal tubule) of the residual nephrons. This type of growth response is called compensatory renal hypertrophy.[1-3] Compensatory renal hypertrophy can occur in kidney donors, kidney transplant recipients, in response to surgical renal ablation (due to renal trauma or tumor), and in virtually all kidney diseases that cause nephron damage and consequently a reduction in the number of functioning nephrons.[1, 2, 4] Although the hypertrophy is presumably to enhance the functional capacity of the residual nephrons to maintain normal renal function, previous studies have suggested that in some cases, compensatory renal hypertrophy may actually be an excessive or maladaptive response that fosters further nephron damage, progressive decline of renal function, and ultimately end stage renal disease.[1-5] To date, however, the molecular signaling mechanism underlying compensatory renal hypertrophy remains poorly understood.

The mechanistic (formerly mammalian) target of rapamycin (mTOR) is an evolutionarily conserved serine/threonine protein kinase that controls protein synthesis, cell growth and metabolism in response to growth factors, nutrients, oxygen, energy levels, and stress in the cell.[6] mTOR forms two structurally and functionally distinct multiprotein complexes: mTOR complex 1 (mTORC1) and mTORC2, in all mammalian cells.[6] Increased mTORC1 activity not only stimulates ribosome biogenesis and protein synthesis but also modulates a range of cellular activities that are essential for cell growth.[7, 8] Unlike mTORC1, mTORC2 neither regulates the phosphorylation of S6 kinase 1 (S6K1) and eukaryotic translation initiation factor (eIF) 4E-binding protein 1 (4E-BP1) nor is sensitive to rapamycin;[9, 10] instead, mTORC2 regulates the class I phosphatidylinositol 3-kinase (PI3K) signaling pathway by directly phosphorylating Akt on the key residue Ser473.[11] However, further studies showed that prolonged rapamycin treatment reduces the levels of mTORC2 by inhibiting the assembly of mTORC2 in some cell types,[12] and more recent studies showed that mTORC1 negatively regulates mTORC2.[13, 14]

Our previous studies demonstrated that unilateral nephrectomy (UNX) increased phosphorylation of both the small ribosomal protein S6 (rpS6) and 4E-BP1 and the content of not only 40S and 60S ribosomal subunits but also 80S monosomes and polysomes in the remaining kidney, suggesting activation of the mTORC1 signaling pathway.[15] Rapamycin blocked UNX-induced phosphorylation of both rpS6 and 4E-BP1, decreased UNX-induced polysome formation, shifted the polysome profile in the direction of monosomes and ribosomal subunits, and inhibited UNX-induced renal hypertrophy, suggesting that mTORC1 activation plays a key role in compensatory renal hypertrophy.[15] We and others have also demonstrated increased mTORC1 activity during renal hypertrophy in response to

diabetes.[16, 17] Diabetic renal hypertrophy is associated with reduced phosphorylation of the AMP-activated protein kinase (AMPK) at Thr172, leading to increased mTORC1 activity.[18] Our more recent studies demonstrated that S6 kinase 1 knockout ($S6K1^{-/-}$) mice exhibited moderately elevated basal levels of rpS6 phosphorylation, which did not increase further in response to hypertrophic stimuli such as UNX. Northern blotting analysis revealed moderately up-regulated S6 kinase 2 (S6K2) expression, presumably accounting for the elevated basal level of rpS6 phosphorylation in the kidneys of $S6K1^{-/-}$ mice. However, homozygous S6K1 knockout did blunt UNX-induced compensatory renal hypertrophy, and rapamycin also inhibited an equivalent degree of renal hypertrophy in wild type mice in response to UNX.[16] These studies indicate that UNX-induced mTORC1 activation selectively activates S6K1 without activating S6K2, thus demonstrating that S6K1, but not S6K2, plays a major role in medicating renal hypertrophy.

However, S6K1 has multiple substrates.[19] For example, S6K1 phosphorylates eEF2K to enhance protein synthesis,[20] and the cell growth regulator SKAR (S6K1 Aly/REF-like target) has also been identified as a substrate for S6K1, but not for S6K2.[21] S6K1 also phosphorylates insulin receptor substrate 1 (IRS1)[22] and mTOR[23] in response to nutrients and growth factors, albeit in a feedback fashion. Of interest, previous studies have shown that mouse embryonic fibroblasts (MEFs) with deficiency in rpS6 phosphorylation are significantly smaller than wild-type MEFs, but their size is not further decreased by rapamycin treatment, suggesting that rpS6 is a critical mTORC1 effector that regulates cell size.[24] Moreover, the small size phenotype is not limited to embryonic cells, since S6 phosphorylation-deficient adult mice also have smaller pancreatic β-cells and smaller myoblasts than their will-type counterparts, respectively.[24, 25] These results suggest that rpS6 phosphorylation plays a physiological role in regulation of cell size.

Although previous studies have demonstrated that activation of the mTORC1-S6K1 signaling pathway is a major mechanism underlying renal hypertrophy,[16-18] the existence of multiple S6K1 substrates warranted our further studies to determine the downstream effector of the mTORC1-S6K1 pathway in renal hypertrophy. Previous studies consistently revealed a marked increase in rpS6 phosphorylation in the remaining kidney in response to UNX.[15, 16] Hence, in the present study we generated a congenic knockin mouse line expressing unphosphorylatable rpS6 and examined the effect of rpS6 phosphorylation deficiency on UNX-induced renal hypertrophy. Our results demonstrated that phosphorylated rpS6 is the downstream effector of the mTORC1-S6K1 signaling pathway, whose activation is necessary for compensatory renal hypertrophy.

## RESULTS

### Generation of congenic rpS6 knockin mice deficient in phosphorylation of the ribosomal protein S6

There are totally five phosphorylatable serine residues in rpS6 at positions 235, 236, 240, 244, and 247, clustered at the carboxyl-terminus that are encoded by the exon 5 of *rpS6* gene and are conserved from *Drosophila* to human.[26, 27] Using site-directed mutagenesis, a targeting vector was constructed to mutate the serine codons within the exon 5 of *rpS6* gene derived from a 129Sv/J library (Stratagene) so all five phosphorylatable serine residues were

replaced with alanine residues in the rpS6 protein, as depicted in Fig. 1a[24] Through homologous recombination in ES cells derived from the R1 (129Sv × 129Sv-CP) mice, the mutated allele of *rpS6* gene was knocked in and chimeric mice were generated. Male chimeras were mated with ICR females to produce heterozygous mutant mice, which were intercrossed to produce homozygous mutant mice, which ended up on 129Sv/J × ICR mixed genetic background.[24] However, a recent study reported that 75% nephrectomy induced severe renal lesions within 2 months only in FVB/N mice but not in other strains such as 129S2/Sv, C57BL/6, DBA/2, (C57BL/6×DBA/2)F1 hybrid, or (C57BL/6×SJL)F1 hybrid mice,[28] which confirmed the previous finding that the response of the kidney to nephrectomy is highly strain-dependent in mice.[29, 30] Therefore, to minimize individual variability and generate a stable mouse line more susceptible to kidney phenotypes in response to nephrectomy, we backcrossed the rpS6 mutant mice that were on 129Sv/J and ICR-mixed background[24] to the inbred FVB/NJ mice (Jackson Laboratory) for 10 generations and produced congenic rpS6 knockin mice expressing unphosphorylatable rpS6 on FVB/NJ background ($rpS6^{P-/-}$), as indicated in Fig.1b, and used their gender-matched wild type littermates as control mice ($rpS6^{P+/+}$) for the subsequent experiments.

We first determined the genotype of the mice by PCR of the genomic DNA from ear-punch biopsy and detected the expected 339-bp band of the mutant allele in both $rpS6^{P+/-}$ and $rpS6^{P-/-}$ mice but not in $rpS6^{P+/+}$ mice while the 639-bp band of wild type allele was detected in both $rpS6^{P+/-}$ and $rpS6^{P+/+}$ mice but not in $rpS6^{P-/-}$ mice (Fig. 1c). Immunoblotting of kidney homogenates with specific phospho-rpS6 antibodies detected both Ser235/236-phosphorylated rpS6 and Ser240/244-phosphorylated rpS6 in $rpS6^{P+/+}$ mice; in contrast, both Ser235/236-phosphorylated rpS6 and Ser240/244-phosphorylated rpS6 were completely deleted in $rpS6^{P-/-}$ mice (Fig. 1d)Immunofluorescence staining further confirmed complete deletion of rpS6 phosphorylation in $rpS6^{P-/-}$ mice and revealed that both Ser235/236-phosphorylated rpS6 and Ser240/244-phosphorylated rpS6 were primarily localized to the renal tubules of $rpS6^{P+/+}$ mice (Fig. 1e). We performed co-immunofluorescence staining for synaptopodin, a marker for podocytes, to highlight podocytes so that the locations of glomeruli relative to renal tubules could be visualized; $rpS6^{P+/+}$ mice and $rpS6^{P-/-}$ mice had similar synaptopodin expression (Fig. 1e). Additional quantitative immunoblotting analysis of synaptopodin confirmed that deletion of rpS6 phosphorylation had no effect on the protein expression level of synaptopodin (Fig. 1d).

## Deletion of rpS6 phosphorylation had no effect on the body weight, renal histology, and kidney function

Previous studies demonstrated that homozygous S6K1 knockout did not affect viability or fertility but had a significant effect on animal growth, resulting in a small mouse phenotype.[31] Here we found that homozygous deletion of rpS6 phosphorylation did not affect the fertility, development, and growth of the mice. Homozygous $rpS6^{P-/-}$ knockin pups were born at expected Mendelian ratios (data not shown) and were indistinguishable from their $rpS6^{P+/+}$ littermates at birth. Even after they became adult, $rpS6^{P-/-}$ mice had a mean body weight similar to that of their gender-matched $rpS6^{P+/+}$ littermates (Fig. 2a). The renal histology of $rpS6^{P-/-}$ mice was also similar to that of $rpS6^{P+/+}$ mice (Fig. 2b).

We also examined the kidney function of rpS6$^{P-/-}$ mice by measuring the blood urea nitrogen (BUN) level and found no difference compared with rpS6$^{P+/+}$ mice (Fig. 2c). Sodium dodecyl sulphate-polyacrylamide gel electrophoresis (SDS-PAGE) followed by Coomassie blue staining did not detect any proteinuria in rpS6$^{P-/-}$ or rpS6$^{P+/+}$ mice (Fig. 2d), although with a loading of only 1 μl urine, SDS-PAGE assay clearly visualized the apparent increases in urinary protein excretion in 2 to 3-week-old podocyte-specific mVps34 knockout mice, which have been shown previously to develop massive proteinuria by 6 weeks of age.[32] In additional experiments, we measured urinary albumin/creatinine ratio and confirmed that there was no proteinuria in rpS6$^{P+/+}$ mice and rpS6$^{P-/-}$ mice in response to either sham or uninephrectomy (UNX) surgery, as indicated by the similar level of urinary albumin/creatinine ratio in all four groups of mice, although the assay showed a significant increase of urinary albumin/creatinine ratio in podocyte-specific mVps34 knockout mice, which were known to develop proteinuria after 2 weeks of age[32] and so used as a positive control group (Fig. 2e).

## Deletion of rpS6 phosphorylation blunted development of compensatory renal hypertrophy in response to UNX

It is well known that UNX-induced increases in kidney weight are primarily the result of increased protein content in cells along the nephron (particularly in the proximal tubule), rather than cell proliferation or increased water content.[1-3, 33, 34] Thus, UNX-induced percent increase in kidney-to-body weight ratio in comparison with sham-operated control animals has been widely used to determine the degree of renal hypertrophy. As shown in Table 1, seven days after right UNX, we observed significant increases in left kidney weight and left kidney weight to body weight ratio in rpS6$^{P+/+}$ mice. Although the left kidney to body weight ratio of rpS6$^{P-/-}$ mice was not statistically different from that of rpS6$^{P+/+}$ mice in the sham-operated group, the mean left kidney weight of rpS6$^{P-/-}$ mice was significantly less than that of rpS6$^{P+/+}$ mice in the UNX group, consequently resulting in decreased left kidney weight/body weight ratio in rpS6$^{P-/-}$ mice compared with that in rpS6$^{P+/+}$ mice in the UNX group. However, the mean body weight of rpS6$^{P-/-}$ mice was not significantly different from that of their rpS6$^{P+/+}$ littermates, either in the sham-operated group or in the UNX group, respectively. Also, the mean left kidney weight of rpS6$^{P-/-}$ mice was not significantly different from that of rpS6$^{P+/+}$ littermates in the sham group (Table1). As shown in Fig. 3a, deletion of rpS6 phosphorylation significantly inhibited the increases in left kidney weight/body weight ratio in response to right UNX. Such an inhibitory effect was confirmed by a significant reduction of the UNX-induced increases in protein/DNA ratio in rpS6$^{P-/-}$ mice compared with that in rpS6$^{P+/+}$ control mice; these data further confirmed that what we observed were hypertrophy, rather than hyperplasia (Fig. 3b).

Previous studies have indicated that compensatory renal hypertrophy is mediated by a cell cycle-dependent mechanism.[35] In a mouse model of UNX, it has been demonstrated that UNX stimulated an increase in the protein/DNA ratio without a change in BrdU incorporation in the remaining kidney, and cdk4/cyclin D kinase activity was progressively increased while cdk2/cyclin E kinase activity was decreased 4-7 days following UNX.[35] In the present study, we also observed increases in cyclin D and decreases in cyclin E in the remaining kidney of rpS6$^{P+/+}$ mice in response to UNX. Of interest, these changes were

attenuated in rpS6$^{P-/-}$ mice subjected to UNX (Fig. 3c). These data revealed that the increases in cyclin D and decreases in cyclin E seen in the rpS6$^{P+/+}$ mice are mediated by UNX-induced rpS6 phosphorylation.

Although without any challenge, the renal histology and function of rpS6$^{P-/-}$ mice were not noticeably different from that of rpS6$^{P+/+}$ mice (Fig. 2), deletion of rpS6 phosphorylation significantly inhibited UNX-induced renal hypertrophy, as indicated by blunted increases in kidney/body weight ratio (Fig. 3a) and protein/DNA ratio (Fig. 3b). In response to UNX, although the other components of the nephrons in the remaining kidney may also hypertrophy, the proximal tubule has been consistently demonstrated to be the nephron segment that undergoes the most prominent hypertrophy.[36-39] Since renal proximal tubules make up 80% of the mass of the kidney, their growth accounts for most of the hypertrophic growth in the kidney.[1-5] In the present study, in additional to using H&E staining to show the renal histology (Fig. 4a), to determine the inhibitory effect of rpS6 phosphorylation deficiency on the hypertrophy of renal proximal tubules and glomeruli, we conducted morphometric analysis in rpS6$^{P-/-}$ mice and rpS6$^{P+/+}$ mice with or without UNX following immunofluorescence staining with fluorescein-labeled *Lotus Tetragonolobus Lectin* (LTL, a specific marker to visualize proximal tubules) and an antibody to synaptopodin (specific for podocytes to visualize glomeruli), as shown in Fig. 4b. We selected and measured the size of renal proximal tubules in three different ways as detailed in the *Methods*. Comparing the areas of the largest proximal tubules (Fig. 4c and Supplementary Fig. S1), the areas of randomly measured proximal tubules (Supplementary Fig. S2a and b), and the diameters of randomly selected circular (transversely cut) proximal tubules (Supplementary Fig. S3a and b) all led to the same conclusion that deletion of rpS6 phosphorylation significantly inhibited UNX-induced proximal tubule hypertrophy.

For morphometric comparison of glomerular size, we measured the areas and calculated the volumes of all glomeruli in each captured image as detailed in the *Methods* and shown in Supplementary Fig. S4a. Surprisingly, deletion of rpS6 phosphorylation numerically, but not statistically, reduced UNX-induced increases in either glomerular areas (Fig. 4d) or glomerular volumes (Supplementary Fig. S4b). Thus, our morphometric data indicate that rpS6 phosphorylation plays an important role in compensatory proximal tubular, but not glomerular, hypertrophy, suggesting that the mechanism of glomerular hypertrophy may not be the same as that of proximal tubular hypertrophy. There were no apparent morphological changes in the interstitium of the kidney in rpS6$^{P+/+}$ mice and rpS6$^{P-/-}$ mice with or without UNX (Fig. 4a).

## Deletion of rpS6 phosphorylation had no effect on UNX-induced mTORC1 activation

Immunoblotting revealed increases in rpS6 phosphorylation at both Ser235/236 and Ser240/244 in rpS6$^{P+/+}$ mice in response to UNX but not in rpS6$^{P-/-}$ mice subjected to either sham-operation or UNX (Fig. 5a). However, the total rpS6 protein level in rpS6$^{P-/-}$ mice remained unchanged, compared with that in rpS6$^{P+/+}$ control littermates, indicating that rpS6 phosphorylation deficiency had no effect on the expression of total rpS6 protein.

Our previous studies also demonstrated that UNX increased the phosphorylation of 4E-BP1, another substrate of mTORC1 kinase activity.[15, 16] There is also evidence that Ser65-

phosphorylated 4E-BP1 dissociates from the eukaryotic translation initiation factor (eIF) 4E and consequently allows eIF4E to bind the 5'-cap structure of mRNA, which is a key step in the initiation of cap-dependent translation and cell proliferation.[8, 40] To evaluate whether mTORC1 was activated in the remaining kidney of rpS6$^{P-/-}$ mice in response to UNX, we measured the level of Ser65-phosphorylated 4E-BP1. As shown in Fig. 5b, UNX stimulated an equivalent increase in 4E-BP1 phosphorylation at Ser65 in both rpS6$^{P-/-}$ and rpS6$^{P+/+}$ mice, indicating that mTORC1 was still activated to the same degree in rpS6$^{P-/-}$ mice as in rpS6$^{P+/+}$ littermates.

To determine the mTOR complex 2 (mTORC2) signaling activities during UNX-induced renal growth, we examined the level of Ser473-phosphorylated Akt, a serine/threonine protein kinase that is also known as protein kinase B (PKB), because previous studies have clearly demonstrated that activated mTORC2 directly phosphorylates Akt specifically at Ser473 residue, and this phosphorylation is required for the full activation of Akt.[11] As shown in Fig. 5c, our results indicated that neither UNX nor deletion of rpS6 phosphorylation affected Akt phosphorylation at Ser473, indicating that the mTORC2-Akt signaling pathway is not involved in UNX-induced renal hypertrophy.

## Rapamycin inhibited 4E-BP1 phosphorylation at Ser65 and rpS6 phosphorylation at Ser235/236/240/244

The mTOR inhibitor, rapamycin, prevented UNX-induced rpS6 phosphorylation at Ser235/236 as well as Ser240/244 in rpS6$^{P+/+}$ mice, although no rpS6 phosphorylation at Ser235/236 or Ser240/244 was detected in either vehicle- or rapamycin-treated rpS6$^{P-/-}$ mice subjected to either sham or UNX surgery (Fig. 6a).

Our previous studies with inbred DBA/2 mice have clearly showed that UNX induces 4E-BP1 phosphorylation at multiple sites including Thr37, Thr46, Thr70, and Ser65 in the remaining kidney, but only the phosphorylation of Ser65 and Thr70 can be completely inhibited by rapamycin, with phosphorylation of Thr46 and Thr37 being resistant to rapamycin treatment.[15] Hence, we utilized this rapamycin-sensitive characteristic of Ser65 phosphorylation in 4E-BP1 to monitor whether the administered rapamycin had effectively blocked mTORC1 signaling activity in the rpS6$^{P-/-}$ knockin mice, since the phosphorylation status of rpS6 could not be used anymore in these mice as a readout for mTORC1 signaling. As shown in Fig. 6b, rapamycin blocked the increased 4E-BP1 phosphorylation at Ser65 in rpS6$^{P-/-}$ mice as well as rpS6$^{P+/+}$ mice in response to UNX but did not inhibit the total 4E-BP1 protein expression level, although rapamycin treatment markedly accelerated the migration of total 4E-BP1 bands, consistent with mTORC1 inhibition-mediated dephosphorylation of 4E-BP1 as reported previously.[15] Of note, even the basal level of 4E-BP1 phosphorylation at Ser65 was blocked by rapamycin, indicating that both the basal level of 4E-BP1 phosphorylation and the UNX-induced 4E-BP1 phosphorylation at Ser65 are mediated by rapamycin-sensitive mTORC1 kinase activity in the remaining kidney (Fig. 6b). In contrast, rapamycin did not affect the level of Ser473 phosphorylated Akt in rpS6$^{P-/-}$ mice and rpS6$^{P+/+}$ mice after either sham-surgery or UNX, indicating that mTORC2 activity was not altered (Fig. 6c).

### Rapamycin had no effect on UNX-induced renal hypertrophy in rpS6$^{P-/-}$ knockin mice

As demonstrated in Figure 3a and b, deletion of rpS6 phosphorylation did not completely prevent the development of compensatory renal hypertrophy in response to UNX, and mTORC1 was still activated in the remaining kidney of rpS6$^{P-/-}$ mice (as indicated by UNX-induced increases in 4E-BP1 phosphorylation shown in Fig. 5b). Therefore, we examined whether preventing mTORC1 activation could block the residual renal hypertrophy seen in rpS6$^{P-/-}$ mice. Our results indicated that administration of rapamycin for 7 days (with the first injection being 2 h before the surgery) following UNX significantly blunted the increases in absolute kidney weight and kidney weight to body weight ratio in rpS6$^{P+/+}$ mice, compared with the UNX-rpS6$^{P+/+}$ mice treated with vehicle alone (Table 2 and Fig. 7a). Rapamycin treatment also significantly reduced UNX-induced increases in protein/DNA ratio in rpS6$^{P+/+}$ mice (Fig. 7b). However, rapamycin failed to completely block right UNX-induced increases in the absolute value of left kidney weight (compared rpS6$^{P+/+}$/UNX/Rapa group with rpS6$^{P+/+}$/Sham/Vehicle group in Table 2) and was unable to completely prevent UNX-induce increases in kidney/body weight ratio (Fig. 7a) or protein/DNA ratio (Fig. 7b) in rpS6$^{P+/+}$ mice. Moreover, rapamycin had no statistically significant effect on the kidney weight/body weight ratio (Table 2 and Fig. 7a) and protein/DNA ratio (Fig. 7b) in rpS6$^{P-/-}$ mice, even though rapamycin did block mTORC1 activation in rpS6$^{P-/-}$ mice, as indicated by the blockade of UNX-induced increases in 4E-BP1 phosphorylation (Fig. 6b). These data suggest that phosphorylated rpS6 is the downstream effector of the mTORC1-S6K1 signaling pathway that mediates the major fraction of compensatory renal hypertrophy seen in rpS6$^{P+/+}$ mice in response to UNX.

## DISCUSSION

The phenomenon of compensatory renal hypertrophy has been observed for more than a century,[41] and significant evidence suggests that excessive compensatory renal hypertrophy may be a maladaptive response that sets the stage for an inexorable progression of further nephron damage, interstitial fibrosis, tubular atrophy, progressive decline of renal function and development of end-stage renal disease, while attenuation of compensatory renal hypertrophy might limit progressive kidney damage[1-5, 42-44]. It is important to emphasize that compensatory renal hypertrophy occurs in virtually all kidney diseases that cause nephron damage and consequently a reduction in functioning nephron number.[1, 2, 4, 43, 45] However, the growth signal and molecular signaling mechanism mediating the onset and extent of compensatory renal hypertrophy remain poorly understood. Here we report that rapamycin-sensitive rpS6 phosphorylation is a major downstream effector of the mTORC1-S6K1 signaling pathway that mediates compensatory renal hypertrophy.

Interestingly, recent studies suggest that cell growth and cell cycle progression are separable and distinct processes.[40, 46, 47] There is a study demonstrating that mTORC1 signals downstream to at least two independent targets, S6K1 and 4E-BP1, that function in translational control to regulate mammalian cell size.[47] Yet, more recent evidence indicates that the eukaryotic translation initiation factor 4E-binding proteins (4E-BPs, which have three family members: 4E-BP1, 2, and 3) mediate the effect of mTORC1 to promote cell proliferation, but not growth (thus regulating the number, but not the size) of mammalian

cells.[40] In contrast to 4E-BPs, increasing evidence indicates that S6K1 plays an important role in regulating both cell growth and organ size in mammals[47-50] Of note, this growth regulatory effect is also true for the S6 kinase in *Drosophila*, as it regulates cell size in a cell-autonomous manner without affecting cell number.[46] Overexpression of S6K1 increased cell size, due to augmented cell growth but not to delayed cell cycle progression.[47] Deletion of S6K1 did not affect myoblast cell proliferation but reduced myoblast cell size to the same extent as that observed with mTORC1 inhibition by rapamycin.[50] In the differentiated state, S6K1-null myotubes had a normal number of nuclei but were significantly smaller, and their hypertrophic response to IGF1, nutrients and membrane-targeted Akt was blunted.[50] Moreover, homozygous S6K1 knockout in mice significantly reduced the size of the animals compared to their wild type littermates.[31] This study resulted in the identification of the S6K1 homologue, S6K2,[31] and subsequent studies demonstrated that mice with homozygous S6K2 deletion tend to be slightly larger while mice lacking both S6K1 and S6K2 genes exhibit a sharp reduction in viability due to perinatal lethality.[49]

Our initial studies with wild type mice alone demonstrated that in kidneys undergoing hypertrophy, phosphorylation of 4E-BP1 was detected at multiple sites including Thr37, Thr46, Thr70, and Ser65.[15] However, phosphorylation of Ser65 and Thr70 was completely prevented by rapamycin, with phosphorylation of Thr46 being less inhibited and that of Thr37 the least inhibited by rapamycin.[15] These observations are consistent with previous reports by others, indicating that phosphorylation of Thr37 and Thr46 is relatively resistant to rapamycin, whereas phosphorylation of Ser65 and Thr70 is rapamycin-sensitive.[51] Our results in the present study showed that genetic deletion of rpS6 phosphorylation significantly inhibited compensatory renal hypertrophy. Furthermore, in $rpS6^{P+/+}$ mice, rapamycin prevented UNX-induced rpS6 phosphorylation at both Ser235/236 and Ser240/244 as well as 4E-BP1 phosphorylation at Ser65 and inhibited the hypertrophy to the same extent as inhibited by the deletion of rpS6 phosphorylation, compared with renal hypertrophy in the $rpS6^{P-/-}$ mice in response to UNX without rapamycin treatment. Moreover, rapamycin treatment of the $rpS6^{P-/-}$ knockin mice failed to induce any additive effect, i.e., rapamycin did not further inhibit the residual renal hypertrophy seen in $rpS6^{P-/-}$ knockin mice in response to UNX, although it did block UNX-induced increases in 4E-BP1 phosphorylation and even blocked the basal 4E-BP1 phosphorylation at Ser65. Thus, our results demonstrate that phosphorylated rpS6 is the downstream effector of mTORC1-S6K1 activation that mediates the major fraction of compensatory renal hypertrophy while a rapamycin-insensitive and rpS6 phosphorylation-independent mechanism mediates the residual portion of compensatory renal hypertrophy seen in the $rpS6^{P-/-}$ knockin mice.

Noteworthy, phosphorylation of 4E-BP1 (also a downstream target of mTORC1) was stimulated to equivalent levels in $rpS6^{P-/-}$ and $rpS6^{P+/+}$ mice in response to UNX, indicating that mTORC1 was still activated to a comparable degree in the $rpS6^{P-/-}$ knockin mice. Moreover, even the basal level of 4E-BP1 phosphorylation at Ser65 was blocked by rapamycin, suggesting that both the basal level of 4E-BP1 phosphorylation at Ser65 and the UNX-induced 4E-BP1 phosphorylation at Ser65 are mediated by rapamycin-sensitive mTORC1 kinase activity. However, a previous study reported that the ATP-competitive mTOR inhibitor, Torin1, directly inhibited both mTORC1 and mTORC2 and impaired cell

growth and proliferation to a far greater degree than rapamycin; these effects were independent of mTORC2 inhibition but dependent on inhibition of rapamycin-resistant functions of mTORC1 that were necessary for cap-dependent translation and suppression of autophagy.[52] These effects were at least partly mediated by mTORC1-dependent and rapamycin-resistant phosphorylation of 4E-BP1.[52] In our mouse model, we found that UNX induced significant increases in protein/DNA ratio, indicating a significantly greater increase in protein content than DNA content in the remaining kidney of $rpS6^{P+/+}$ mice (Fig. 3b). We also observed that UNX induced increases in cyclin D1 and decreases in cyclin E1 (Fig. 3c), consistent with previously documented cell cycle-dependent kidney cell growth, with minimal cell cycle transition from G1 phase to DNA synthesis (S phase), during compensatory renal hypertrophy.[35, 53] These UNX-induced alterations in the remaining kidney were significantly attenuated by deletion of rpS6 phosphorylation (Fig. 3b and c). Thus, our data support the notion that rpS6 phosphorylation mediates the well-recognized phenomenon that the increase in protein synthesis and thereby cell size, but not cell number, is the predominant factor causing compensatory renal hypertrophy.[1-5] However, our data in the present study cannot completely rule out a potential requirement of 4E-BP1 in concert with S6K1-mediated rpS6 phosphorylation in the development of hypertrophic renal growth. Of interest, 4E-BP1 knockout mice are viable and fertile with normal life span.[54] Since increment in 4E-BP1 phosphorylation following mTORC1 activation is linked to cell proliferation, at least in cultured cells such as HEK-293T cells and mouse embryonic fibroblasts (MEFs),[40, 52] and cell proliferation is also a contributing factor, albeit very minor, in compensatory renal hypertrophy,[1-5] future studies utilizing 4E-BP1 knockout mice, along with the $rpS6^{P-/-}$ knockin mice, should allow us to address the importance of 4E-BP1 and the mechanism of the minor cell proliferation in compensatory renal hypertrophy.

Upon entry into mammalian cells, rapamycin forms a complex with the immunophilin FK506 binding protein 12 (FKBP12). This complex subsequently binds to the FKBP12-rapamycin-binding (FRB) domain of mTOR within mTORC1 and inhibits the kinase activity of mTORC1; in contrast, the mTOR in mTORC2, which phosphorylates its downstream effector Akt on Ser473 and so activates Akt,[11] does not bind rapamycin-FKBP12 and has been demonstrated to be rapamycin-insensitive,[10] thus rapamycin is commonly accepted as a specific inhibitor for mTORC1. However, there is evidence that prolonged rapamycin treatment inhibits mTORC2 assembly and Akt in a cell type-specific manner,[12] and a more recent study showed that chronic treatment with rapamycin at 2 mg/kg/day by intraperitoneal injection for 14-28 days disrupted the association of mTOR with both Raptor (a core component of mTORC1) and Rictor (rapamycin-insensitive companion of mTOR), a key component that distinguishes mTORC2 from mTORC1, and impaired insulin-mediated suppression of hepatic gluconeogenesis.[55] Of note, a high dosage of mTOR inhibitors had been reported to induce focal segmental glomerulosclerosis and proteinuria in renal transplant patients,[56, 57] and knocking out both alleles of the *Mtor* gene in mouse renal glomerular podocytes had been shown to cause massive proteinuria and renal failure.[58] The majority of compensatory renal hypertrophy occurs within 7 days after removal of contralateral kidney.[15] Accordingly, we chose to give a low dosage of rapamycin (1 mg/kg once every 2 days for 7 days by intraperitoneal injection, with the first injection

being 2 h before the surgery) to the mice used in the present study that were all on FVB/NJ background (this genetic background makes the mice more susceptible to kidney phenotype[28-30]). Our results revealed that such a low dosage and short-term rapamycin treatment was sufficient to completely block UNX-induced increases in Ser65-phosphorylated 4E-BP1 and Ser235/236/240/244-phosphorylated rpS6, which are the downstream targets of mTORC1 and S6K1 kinase activities, respectively.[6] However, such a treatment had no effect on Akt phosphorylation at Ser473, which is the phosphorylation site of mTORC2 kinase activity,[11] in the kidneys of $rpS6^{P-/-}$ and $rpS6^{P+/+}$ mice subjected to either sham surgery or UNX. Importantly, the rapamycin treatment significantly inhibited UNX-induced renal hypertrophy in $rpS6^{P+/+}$ mice but did not block the residual renal hypertrophy induced by UNX in $rpS6^{P-/-}$ mice. Moreover, neither sham-surgery nor UNX altered Ser473-phosphorylated Akt levels. Thus, our results indicate that the low dosage and short-term rapamycin treatment used in current study inhibited UNX-induced renal hypertrophy by blocking mTORC1 signaling to rpS6 phosphorylation; this is consistent with the conclusion that UNX-induced renal hypertrophy is mediated by activation of mTORC1, but not mTORC2. Noteworthy, a very recent study revealed that even long-term rapamycin treatment (from ages 4 through 12 weeks) but at 1 mg/kg per day (administered intragastrically) significantly inhibited rpS6 phosphorylation but did not alter the level of Ser473-phosphorylated Akt in the kidney.[59] Thus, it appears that the effect of rapamycin on mTORC2 may vary considerably, depending on the duration of rapamycin treatment,[12] but probably even more on the dosage of rapamycin used and the cell types and perhaps the genetic background of mouse strains studied.[12, 55, 59] Therefore, in relation to the clinical practice our findings prompt us to highly recommend the lowest possible dosage of rapamycin treatment for renal transplant patients.

In the present study, we also observed that deletion of rpS6 phosphorylation partially inhibited UNX-induced increases in cyclin D1 and decreases in cyclin E1 in the remaining kidney, revealing a key role for rpS6 phosphorylation in regulation of cell cycle-associated kidney growth. How can rpS6 phosphorylation regulate the expression of cyclin D1 and cyclin E1? In this regard, there is evidence that cyclin D1 is a key mediator of increased protein synthesis and cell growth downstream of rapamycin-sensitive mTORC1 activation,[60] and activated mTORC1 is known to directly phosphorylate S6K1 at the rapamycin-sensitive Thr389 to activate S6K1,[9, 10, 61] which is the major kinase responsible for rapamycin-sensitive rpS6 phosphorylation.[62] Furthermore, a recent study demonstrated that S6K1 and S6K2 double knockout ($S6K1^{-/-};S6K2^{-/-}$) inhibits feeding-induced gene transcription for over 75% of ribosome biogenesis factors and more importantly, the reduced transcriptional promoter activity of ribosome biogenesis genes in $S6K1^{-/-};S6K2^{-/-}$ cells is also observed in $rpS6^{P-/-}$ cells.[63] Moreover, the cellular abundance of proteins (including specific proteins, groups of proteins with shared characteristic translation regulatory motifs, and overall protein abundance) in mammalian cells is also controlled at the level of translation.[64] Therefore, in light of the observations in current study, it would be of prime importance to explore the involvement of rpS6 phosphorylation in regulation of the expression of specific genes, such as those encoding cyclin D1 and cyclin E1, at both translational and transcriptional levels. For the present time, we cannot rule out a direct effect of rpS6 phosphorylation on the regulation of cyclin D1 and cyclin E1, although reduced expression

of cyclin D1 might be induced by rpS6 phosphorylation-associated defects in ribosome biogenesis while the slightly increased expression of cyclin E1 might result from ribosome biogenesis deficiency-induced activation of a cell cycle checkpoint mechanism.[65] However, the precise mechanism underlying rpS6 regulation of cyclin D1 and cyclin E1 requires more focused further investigation in future studies. Of note, we found that the cyclin E1 level in the $rpS6^{P-/-}$ mice subjected to UNX was still relatively lower than that of sham-operated $rpS6^{P-/-}$ and $rpS6^{P+/+}$ mice and was presumably still lower than the threshold required for the cells to transit from G1 phase into S phase. These findings are consistent with previous studies demonstrating that renal hypertrophy is regulated by a cell cycle-dependent mechanism in which cyclin-dependent kinase (CDK)4/cyclin D is activated without a subsequent engagement of CDK2/cyclin E.[35, 53] In addition, the activity of CDK/cyclin complexes is modulated by CDK inhibitors (such as p21Cip1 and p27Kip1[66-68]) and TGF-β.[69-71] Thus, the cell cycle is arrested in late G1 without progression into S phase, consequently resulting in hypertrophy rather than hyperplasia.[35, 53, 70, 71] These studies of cell cycle-dependent mechanisms are complementary to our finding of a role for rpS6 phosphorylation in compensatory renal hypertrophy in the present study and our findings of a role for S6K1, but not S6K2, in mediating mTORC1-dependent hypertrophic renal growth in our previous studies,[15, 16] because the studies of CDK/cyclins and CDK inhibitors explain why cells undergo hypertrophy rather than hyperplasia, while our studies delineate the mTORC1-S6K1-rpS6 signaling pathway that mediates the increased protein synthesis and drives the cell to grow in size and mass for the development of renal hypertrophy.

In summary, our current study provides the first definitive genetic evidence and pharmacological data demonstrating that phosphorylated rpS6 is a major downstream effector of the mTORC1-S6K1 pathway that mediates the major fraction of compensatory renal hypertrophy. Our study also uncovered that rpS6 phosphorylation mediates the increased cyclin D1 and decreased cyclin E1 levels that underlie the hypertrophic nature of nephron loss-induced compensatory renal growth. Moreover, rapamycin prevented mTORC1 activation and blocked UNX-induced 4E-BP1 phosphorylation but failed to inhibit the residual renal hypertrophy seen in the $rpS6^{P-/-}$ knockin mice in response to contralateral nephrectomy. Future studies are required to determine the mechanism underlying this residual portion of compensatory renal hypertrophy that is independent of rpS6 phosphorylation.

## MATERIALS AND METHODS

### Chemicals and antibodies

Antibodies against total rpS6, phospho-rpS6, Cyclin D1, Cyclin E1, and phospho-4E-BP1 were from Cell Signaling Technology (Beverly, MA). Fluorescein Lotus-tetragonolobus Lectin (LTL) was purchased from Vector Laboratories Inc, (Burlingame, CA). Anti-synaptopodin antibody was from Acris Antibodies GmbH (San Diego, CA). Anti-rabbit HRP and anti-mouse HRP secondary antibodies, anti-rabbit dyLight 488 were from Vector laboratories (Burlingame, CA). Anti-mouse Alexa 594 was from Invitrogen Life Technologies (Carlsbad, CA). Rapamycin was purchased from LC Laboratories (Woburn,

MA). Antibodies to β-actin and other chemical reagents were purchased from Sigma-Aldrich (St. Louis, MO).

### Generation of congenic *S6$^{P-/-}$ knockin* mice to delete S6 phosphorylation

Animals were housed at the Georgia Regent University veterinary facility. Animal care and all experimental procedures were approved by Georgia Regent University Animal Care and Usage Committee and complied with the guidelines of National Institutes of Health. *rpS6$^{P-/-}$* knockin mice were generated by homologous recombination in 129Sv/J ES cells to knock in an exon 5-mutant allele of S6 gene, in which the codons for all phosphorylatable serines (Ser235, Ser236, Ser240, Ser244, and Ser247) were mutated to code for alanines, with an insertion of an EcoRV site immediately downstream of the coding sequence to facilitate subsequent genotyping. Male chimera derived from correctly targeted ES clones were crossed with ICR females to produce heterozygous S6 knockin mice, which were intercrossed to produce homozygous S6 knockin mice on 129Sv/J x ICR mixed background, as described previously.[24] These mice were backcrossed onto the inbred FVB/NJ strain for 10 generations. The resultant *rpS6$^{P+/-}$* offspring were intercrossed to generate homozygous congenic S6 knockin mice expressing unphosphorylatable ribosomal protein rpS6 (rpS6$^{P-/-}$) on FVB/NJ background and rpS6$^{P+/+}$ wild type littermates (for control). Genotyping was accomplished by PCR using primer pairs spanning the mutated region: 5'-GTCATCCAGCATGGGTGCTG-3' and 5'-GGCTGATACCTTTTGGGACAG-3'. PCR were performed at 95°C for 5 min followed by 95°C for 30 s, 60°C for 30 s, and 72°C for 60 s for 30 cycles, with an additional 7-min extension at 72°C. The PCR product was digested with EcoRV to identify those carrying the mutant allele.

### Surgical procedures

Compensatory renal hypertrophy was induced by right nephrectomy (UNX) as we have previously described.[15] rpS6$^{P-/-}$ and rpS6$^{P+/+}$ mice at 8 weeks of age were utilized. Briefly, under aseptic conditions, UNX was performed through a right flank incision, sparing the adrenal gland, under anesthesia using pentobarbital sodium (50 mg/kg intraperitoneal injection). Left kidneys of right sham-nephrectomized (Sham) mice were used as controls for UNX mice. Sham consisted of anesthesia, flank incision, delivery of the right kidney through the incision, and return to the retroperitoneum. The hypertrophy was evaluated after completely removing the fibrous renal capsule along with the surrounding fatty tissues and renal pedicle from left kidney and mTORC1 signaling activity determined 7 days after the surgery.

### Immunoblotting analysis

Immunoblotting procedures were performed as we described previously.[72] Briefly, left kidneys were decapsulated, and cortices were isolated, cut into pieces, and washed twice with ice-cold PBS, followed by homogenization in the lysis buffer described previously.[72] Renal cortical lysates were clarified at 10,000 g for 15 min at 4°C, and protein concentrations were determined by the Bradford protein assay (Bio-Rad Laboratories, Hercules, CA). Equal amounts of protein were loaded onto 7 to 15% SDS-PAGE, transferred onto polyvinylidene difluoride membranes, probed with the indicated primary

antibody and the appropriate secondary antibody conjugated with HRP, and the immune complexes were detected by a peroxidase- catalyzed enhanced chemiluminescence detection system (Clarity™ Western ECL Substrate, Bio-Rad Laboratory Inc.), and visualized with Bio-Rad image system (ChemiDoc™ MP Imaging system).

### Immunofluorescence staining

Immunofluorescence staining was performed as we previously described.[32] Briefly, kidneys were dissected and fixed in 4% paraformaldehyde. The fixed kidneys were dehydrated through a graded series of ethanol, embedded in paraffin, sectioned (5 μm), and mounted on glass slides. The kidney sections were subjected to antigen retrieval followed by blocking with 2.5% BSA in PBS; the sections were incubated with primary antibodies specifically against Ser235/236-phosphorylated rpS6 (1:200), Ser240/244-phosphorylated rpS6 (1:200), synaptopodin (1:200), overnight at 4°C, and then incubated with Alexa Fluor 594 or dyLight 488-conjugated secondary antibodies or the fluorescein-labeled proximal tubule marker, *Lotus-tetragonolobus Lectin* (LTL) for 1 hour. Nuclei were counterstained with DAPI. Images were captured by using an Olympus D73 fluorescence microscope and Exi-blue digital camera (made in Canada).

### Measurement of blood urea nitrogen

Blood urea nitrogen (BUN) levels were measured as previously described.[16] Briefly, seven days after UNX when the mice were euthanized to determine renal hypertrophy and mTORC1 signaling activity, blood samples were collected and blood urea nitrogen (BUN) levels were immediately measured according to the instruction of the commercially available kit, Liquid Urea Nitrogen Reagent Set (Pointe Scientific, Lincoln Park, MI).

### Measurement of urinary albumin and creatinine

Urine samples from $rpS6^{P-/-}$ mice and $rpS6^{P+/+}$ mice were collected for the measurement of urinary albumin-to-creatinine ratio, with urine samples from podocyte-specific mVps34 knockout mice at 2-3 weeks of age as positive control (our recent study revealed that these knockout mice develop proteinuria after 2 weeks of age[32]). Urine albumin concentration was determined by competitive enzyme-linked immunosorbent assay using an Albuwell M kit (Exocell, Philadelphia, PA). Urine creatinine concentration was measured by Jaffe's reaction of alkaline picrate with creatinine using a Creatinine Companion kit (Exocell, Philadelphia, PA). All measurements were performed in triplicate, and the ratio of urinary albumin to creatinine (micrograms per milligram) was calculated. Results are expressed as the means ± SEM ($n$=5).

### Measurement of protein/DNA ratios

Renal cortex (0.08 g per sample) was homogenized in a 1.5-ml lysis buffer that contained 0.02% SDS, 150 mM NaCl, and 15 mM Na citrate, followed by a 10-fold dilution. DNA determination was performed in triplicate as described previously.[15, 73] Briefly, aliquots of each homogenate were incubated in a 96-well plate at 37°C for 1 h. After addition of 100 μl of 1.0 μg/ml bisbenzimidazole fluorescent dye Hoechst 33258 (Sigma), the samples were read at excitation λ360 nm, emission λ460 nm using a multi-mode microplate reader-

Fluostar Omega (BMG Labtech Inc, Cary NC). Aliquots of the same homogenates were used to determine protein concentration by the Bradford protein assay (Bio-Rad Laboratories). The protein/DNA ratios were calculated, and data were presented as percentage increases compared with sham-operated or vehicle-injected control mice.

### Morphometric analysis of renal proximal tubular and glomerular size

Seven days after rpS6$^{P-/-}$ mice and their rpS6$^{P+/+}$ littermates were subjected to right UNX or Sham surgery, left kidneys were removed and fixed in 4% paraformaldehyde for paraffin-embedded kidney sections at a thickness of 5 microns (5 μm). The kidney sections used for double immunofluorescence staining with fluorescein-labeled *Lotus tetragonolobus Lectin* (LTL, a specific marker for renal proximal tubules) and synaptopodin (specific for podocytes to visualize glomeruli as podocytes are highly specialized visceral epithelial cells that intricately wrap around the outer aspect of the glomerular basement membrane on the surface of glomerular capillary tuft). It would be too tedious and unnecessary to measure each and every tubular compartment in the stained kidney sections; therefore, we randomly captured 5 images at the original magnification of 100× from the LTL-positive region (including the renal cortex containing the S1 and S2 segments of the proximal tubules and the outer stripe of outer medulla containing the S3 segment of the proximal tubules) for each kidney section using the OLYMPUS IX73 inverted 2-deck platform IX73 microscope system running on the CellSens Standard software. Thus, totally 25 microscopic images were collected for each group (5 images/mouse with 5 mice/group).

From each image, we selected the renal proximal tubules in three different ways to measure their size: 1) we visually selected the largest 15 proximal tubules, measured their areas as shown in Supplementary Fig. S1, and selected the top 10 largest proximal tubules (based on the sorted values of the measured 15 tubules) for comparison among 4 different groups (the mean proximal tubular area compared were from the measures of totally 250 proximal tubules per group: the top 10 largest LTL-positive tubules per image × 25 images per group) as shown in Fig. 4c; 2) we randomly measured 10 LTL-positive renal proximal tubules for each image and thus also entered the area values of 250 proximal tubules per group for calculation and comparison of the mean proximal tubular area (Supplementary Fig. S2); and 3) we measured the diameters of randomly selected 10 circular (transversely cut) proximal tubules per image and entered the diameter values of 250 circular proximal tubules from each group for comparison (Supplementary Fig. S3).

For morphometric comparison of glomerular size, we first measured the areas of all glomeruli highlighted by positive synaptopodin staining in each microscopic image using Olympus cellSens Entry software as shown in Supplementary Fig. S4a, and compared the mean areas of all glomeruli from totally 25 images for each group (Fig. 4d). Then considering that comparing the areas of the 2 dimensional glomeruli that we were able to measure in kidney sections could underestimate the size difference of actual glomeruli, because glomeruli are generally considered a 3 dimensional sphere, which should have a volume of $4/3\pi r^3$ (where the radius $r$ is cubed and the product multiplied by 4/3, rather than the radius $r$ only squared when a glomerular area is calculated, presumably using the formula of a circular glomerular area is only $\pi r^2$); therefore, we solved for the radius from

the area value of each measured glomerulus and calculated and compared their mean volumes (Supplementary Fig. S4b).

### Statistics

Data are presented as means ± SE for at least three separate experiments (each in triplicate or duplicate). An unpaired t-test was used for statistical analysis, and ANOVA and Bonferroni t-test were used for multiple-group comparisons using Prism 6 (GraphPad Software, http://www.graphpad.com/scientific-software/prism/). $P < 0.05$ was considered statistically significant.

## Supplementary Material

Refer to Web version on PubMed Central for supplementary material.

## Acknowledgments

This work was supported by funds from National American Heart Association Scientist Development Grant 0630274N, a Vanderbilt Diabetes Research and Training Center Pilot & Feasibility Grant 2P60DK020593, Academic Program Support funds from Vanderbilt University School of Medicine, Startup funds from Medical College of Georgia, Georgia Regents University Augusta, and funds from National Institutes of Health R01 Grant DK83575 (to J.-K. Chen).

## References

1. Preisig, PA. Renal hypertrophy and hyperplasia. In: Selden, DW.; Giebisch, G., editors. The Kidney. 3. Vol. 1. Lippincott Williams & Wilkins; Philadelphia: 2000. p. 727-748.
2. Brenner BM. Remission of renal disease: recounting the challenge, acquiring the goal. J Clin Invest. 2002; 110:1753–1758. [PubMed: 12488422]
3. Fine LG, Norman J. Cellular events in renal hypertrophy. Annu Rev Physiol. 1989; 51:19–32. [PubMed: 2469382]
4. Hostetter TH. Progression of renal disease and renal hypertrophy. Annu Rev Physiol. 1995; 57:263–278. [PubMed: 7778868]
5. Norman, JT.; Fine, LG. Renal growth and hypertrophy. In: Massry, SG.; Glassock, RJ., editors. Textbook of Nephrology. Williams & Wilkins; Baltimore: 1995. p. 146-158.
6. Laplante M, Sabatini DM. mTOR signaling in growth control and disease. Cell. 2012; 149:274–293. [PubMed: 22500797]
7. Schmelzle T, Hall MN. TOR, a central controller of cell growth. Cell. 2000; 103:253–262. [PubMed: 11057898]
8. Gingras AC, Raught B, Sonenberg N. mTOR signaling to translation. Curr Top Microbiol Immunol. 2004; 279:169–197. [PubMed: 14560958]
9. Sarbassov DD, Ali SM, Kim DH, et al. Rictor, a novel binding partner of mTOR, defines a rapamycin-insensitive and raptor-independent pathway that regulates the cytoskeleton. Current biology : CB. 2004; 14:1296–1302. [PubMed: 15268862]
10. Jacinto E, Loewith R, Schmidt A, et al. Mammalian TOR complex 2 controls the actin cytoskeleton and is rapamycin insensitive. Nature cell biology. 2004; 6:1122–1128. [PubMed: 15467718]
11. Sarbassov DD, Guertin DA, Ali SM, et al. Phosphorylation and regulation of Akt/PKB by the rictor-mTOR complex. Science. 2005; 307:1098–1101. [PubMed: 15718470]
12. Sarbassov DD, Ali SM, Sengupta S, et al. Prolonged rapamycin treatment inhibits mTORC2 assembly and Akt/PKB. Mol Cell. 2006; 22:159–168. [PubMed: 16603397]

13. Liu P, Gan W, Inuzuka H, et al. Sin1 phosphorylation impairs mTORC2 complex integrity and inhibits downstream Akt signalling to suppress tumorigenesis. Nature cell biology. 2013; 15:1340–1350. [PubMed: 24161930]
14. Humphrey SJ, Yang G, Yang P, et al. Dynamic adipocyte phosphoproteome reveals that Akt directly regulates mTORC2. Cell metabolism. 2013; 17:1009–1020. [PubMed: 23684622]
15. Chen JK, Chen J, Neilson EG, et al. Role of mammalian target of rapamycin signaling in compensatory renal hypertrophy. J Am Soc Nephrol. 2005; 16:1384–1391. [PubMed: 15788477]
16. Chen JK, Chen J, Thomas G, et al. S6 Kinase 1 Knockout Inhibits Uninephrectomy- or Diabetes-induced Renal Hypertrophy. Am J Physiol Renal Physiol. 2009; 297:F585–593. [PubMed: 19474189]
17. Sakaguchi M, Isono M, Isshiki K, et al. Inhibition of mTOR signaling with rapamycin attenuates renal hypertrophy in the early diabetic mice. Biochem Biophys Res Commun. 2006; 340:296–301. [PubMed: 16364254]
18. Lee MJ, Feliers D, Mariappan MM, et al. A role for AMP-activated protein kinase in diabetes-induced renal hypertrophy. Am J Physiol Renal Physiol. 2007; 292:F617–627. [PubMed: 17018841]
19. Meyuhas O, Dreazen A. Ribosomal protein S6 kinase from TOP mRNAs to cell size. Progress in molecular biology and translational science. 2009; 90:109–153. [PubMed: 20374740]
20. Wang X, Li W, Williams M, et al. Regulation of elongation factor 2 kinase by p90(RSK1) and p70 S6 kinase. EMBO J. 2001; 20:4370–4379. [PubMed: 11500364]
21. Richardson CJ, Broenstrup M, Fingar DC, et al. SKAR is a specific target of S6 kinase 1 in cell growth control. Current biology : CB. 2004; 14:1540–1549. [PubMed: 15341740]
22. Um SH, Frigerio F, Watanabe M, et al. Absence of S6K1 protects against age- and diet-induced obesity while enhancing insulin sensitivity. Nature. 2004; 431:200–205. [PubMed: 15306821]
23. Holz MK, Blenis J. Identification of S6 kinase 1 as a novel mammalian target of rapamycin (mTOR)-phosphorylating kinase. J Biol Chem. 2005; 280:26089–26093. [PubMed: 15905173]
24. Ruvinsky I, Sharon N, Lerer T, et al. Ribosomal protein S6 phosphorylation is a determinant of cell size and glucose homeostasis. Genes Dev. 2005; 19:2199–2211. [PubMed: 16166381]
25. Ruvinsky I, Katz M, Dreazen A, et al. Mice deficient in ribosomal protein S6 phosphorylation suffer from muscle weakness that reflects a growth defect and energy deficit. PloS one. 2009; 4:e5618. [PubMed: 19479038]
26. Krieg J, Hofsteenge J, Thomas G. Identification of the 40 S ribosomal protein S6 phosphorylation sites induced by cycloheximide. J Biol Chem. 1988; 263:11473–11477. [PubMed: 3403539]
27. Fumagalli, S.; Thomas, G. S6 phosphorylation and signal transduction. In: Sonenberg, N.; Hershey, JWB.; Mathews, MB., editors. Translational Control of Gene Expression. Cold Spring Harbor Laboratory Press; Cold Spring Harbor, New York: 2000. p. 695-717.
28. Laouari D, Burtin M, Phelep A, et al. TGF-alpha mediates genetic susceptibility to chronic kidney disease. J Am Soc Nephrol. 2011; 22:327–335. [PubMed: 21183591]
29. Esposito C, He CJ, Striker GE, et al. Nature and severity of the glomerular response to nephron reduction is strain-dependent in mice. Am J Pathol. 1999; 154:891–897. [PubMed: 10079267]
30. Ma LJ, Fogo AB. Model of robust induction of glomerulosclerosis in mice: importance of genetic background. Kidney Int. 2003; 64:350–355. [PubMed: 12787428]
31. Shima H, Pende M, Chen Y, et al. Disruption of the p70(s6k)/p85(s6k) gene reveals a small mouse phenotype and a new functional S6 kinase. Embo J. 1998; 17:6649–6659. [PubMed: 9822608]
32. Chen J, Chen MX, Fogo AB, et al. mVps34 deletion in podocytes causes glomerulosclerosis by disrupting intracellular vesicle trafficking. J Am Soc Nephrol. 2013; 24:198–207. [PubMed: 23291473]
33. Shechter P, Shi JD, Rabkin R. Renal tubular cell protein breakdown in uninephrectomized and ammonium chloride-loaded rats. J Am Soc Nephrol. 1994; 5:1201–1207. [PubMed: 7873730]
34. Rabkin R, Shechter P, Shi JD, et al. Protein turnover in the hypertrophying kidney. Miner Electrolyte Metab. 1996; 22:153–156. [PubMed: 8676809]
35. Liu B, Preisig PA. Compensatory renal hypertrophy is mediated by a cell cycle-dependent mechanism. Kidney Int. 2002; 62:1650–1658. [PubMed: 12371965]

36. Arataki M. Experimental researches on the compensatory enlargement of the surviving kidney afer unilateral nephrectomy (albino rat). Am J Anat. 1926; 36:437–450.
37. Hayslett JP, Kashgarian M, Epstein FH. Functional correlates of compensatory renal hypertrophy. J Clin Invest. 1968; 47:774–799. [PubMed: 5641618]
38. Oliver J. New directions in renal morphology: A method, its results and its future. Harvey Lecture. 1944; 40:102–155.
39. Trizna W, Yanagawa N, Bar-Khayim Y, et al. Functional profile of the isolated uremic nephron. Evidence of proximal tubular “memory” in experimental renal disease. J Clin Invest. 1981; 68:760–767. [PubMed: 7276170]
40. Dowling RJ, Topisirovic I, Alain T, et al. mTORC1-mediated cell proliferation, but not cell growth, controlled by the 4E-BPs. Science. 2010; 328:1172–1176. [PubMed: 20508131]
41. Nowinski, WW. Early history of renal hypertrophy. In: Nowinski, WW.; Goss, RJ., editors. Compesatory renal hypertrophy. Scademic Press; New York and London: 1969. p. 1-8.
42. Hostetter TH, Olson JL, Rennke HG, et al. Hyperfiltration in remnant nephrons: a potentially adverse response to renal ablation. Am J Physiol. 1981; 241:F85–93. [PubMed: 7246778]
43. Fries JW, Sandstrom DJ, Meyer TW, et al. Glomerular hypertrophy and epithelial cell injury modulate progressive glomerulosclerosis in the rat. Lab Invest. 1989; 60:205–218. [PubMed: 2915515]
44. Daniels BS, Hostetter TH. Adverse effects of growth in the glomerular microcirculation. Am J Physiol. 1990; 258:F1409–1416. [PubMed: 2337156]
45. Brenner BM, Mackenzie HS. Nephron mass as a risk factor for progression of renal disease. Kidney Int Suppl. 1997; 63:S124–127. [PubMed: 9407439]
46. Montagne J, Stewart MJ, Stocker H, et al. Drosophila S6 kinase: a regulator of cell size. Science. 1999; 285:2126–2129. [PubMed: 10497130]
47. Fingar DC, Salama S, Tsou C, et al. Mammalian cell size is controlled by mTOR and its downstream targets S6K1 and 4EBP1/eIF4E. Genes Dev. 2002; 16:1472–1487. [PubMed: 12080086]
48. Kwon CH, Zhu X, Zhang J, et al. mTor is required for hypertrophy of Pten-deficient neuronal soma in vivo. Proc Natl Acad Sci U S A. 2003; 100:12923–12928. [PubMed: 14534328]
49. Pende M, Um SH, Mieulet V, et al. S6K1(-/-)/S6K2(-/-) mice exhibit perinatal lethality and rapamycin-sensitive 5’-terminal oligopyrimidine mRNA translation and reveal a mitogen-activated protein kinase-dependent S6 kinase pathway. Mol Cell Biol. 2004; 24:3112–3124. [PubMed: 15060135]
50. Ohanna M, Sobering AK, Lapointe T, et al. Atrophy of S6K1(-/-) skeletal muscle cells reveals distinct mTOR effectors for cell cycle and size control. Nature cell biology. 2005; 7:286–294. [PubMed: 15723049]
51. Fadden P, Haystead TA, Lawrence JC Jr. Identification of phosphorylation sites in the translational regulator, PHAS-I, that are controlled by insulin and rapamycin in rat adipocytes. J Biol Chem. 1997; 272:10240–10247. [PubMed: 9092573]
52. Thoreen CC, Kang SA, Chang JW, et al. An ATP-competitive mammalian target of rapamycin inhibitor reveals rapamycin-resistant functions of mTORC1. J Biol Chem. 2009; 284:8023–8032. [PubMed: 19150980]
53. Huang HC, Preisig PA. G1 kinases and transforming growth factor-beta signaling are associated with a growth pattern switch in diabetes-induced renal growth. Kidney Int. 2000; 58:162–172. [PubMed: 10886561]
54. Tsukiyama-Kohara K, Poulin F, Kohara M, et al. Adipose tissue reduction in mice lacking the translational inhibitor 4E-BP1. Nat Med. 2001; 7:1128–1132. [PubMed: 11590436]
55. Lamming DW, Ye L, Katajisto P, et al. Rapamycin-induced insulin resistance is mediated by mTORC2 loss and uncoupled from longevity. Science. 2012; 335:1638–1643. [PubMed: 22461615]
56. Letavernier E, Bruneval P, Mandet C, et al. High sirolimus levels may induce focal segmental glomerulosclerosis de novo. Clin J Am Soc Nephrol. 2007; 2:326–333. [PubMed: 17699432]

57. Stallone G, Infante B, Pontrelli P, et al. Sirolimus and proteinuria in renal transplant patients: evidence for a dose-dependent effect on slit diaphragm-associated proteins. Transplantation. 2011; 91:997–1004. [PubMed: 21364499]
58. Cina DP, Onay T, Paltoo A, et al. Inhibition of MTOR Disrupts Autophagic Flux in Podocytes. J Am Soc Nephrol. 2012; 23:412–420. [PubMed: 22193387]
59. Chen Z, Dong H, Jia C, et al. Activation of mTORC1 in collecting ducts causes hyperkalemia. J Am Soc Nephrol. 2014; 25:534–545. [PubMed: 24203997]
60. Nelsen CJ, Rickheim DG, Tucker MM, et al. Evidence that cyclin D1 mediates both growth and proliferation downstream of TOR in hepatocytes. J Biol Chem. 2003; 278:3656–3663. [PubMed: 12446670]
61. Pearson RB, Dennis PB, Han JW, et al. The principal target of rapamycin-induced p70s6k inactivation is a novel phosphorylation site within a conserved hydrophobic domain. Embo J. 1995; 14:5279–5287. [PubMed: 7489717]
62. Stewart MJ, Thomas G. Mitogenesis and protein synthesis: a role for ribosomal protein S6 phosphorylation? Bioessays. 1994; 16:809–815. [PubMed: 7840758]
63. Chauvin C, Koka V, Nouschi A, et al. Ribosomal protein S6 kinase activity controls the ribosome biogenesis transcriptional program. Oncogene. 2014; 33:474–483. [PubMed: 23318442]
64. Schwanhausser B, Busse D, Li N, et al. Global quantification of mammalian gene expression control. Nature. 2011; 473:337–342. [PubMed: 21593866]
65. Elledge SJ. Cell cycle checkpoints: Preventing an identity crisis. Science. 1996; 274:1664–1672. [PubMed: 8939848]
66. Bell SP, Dutta A. DNA replication in eukaryotic cells. Annu Rev Biochem. 2002; 71:333–374. [PubMed: 12045100]
67. Monkawa T, Hiromura K, Wolf G, et al. The hypertrophic effect of transforming growth factor-beta is reduced in the absence of cyclin-dependent kinase-inhibitors p21 and p27. J Am Soc Nephrol. 2002; 13:1172–1178. [PubMed: 11961004]
68. Wolf G, Jablonski K, Schroeder R, et al. Angiotensin II-induced hypertrophy of proximal tubular cells requires p27Kip1. Kidney Int. 2003; 64:71–81. [PubMed: 12787397]
69. Wolf G, Mueller E, Stahl RA, et al. Angiotensin II-induced hypertrophy of cultured murine proximal tubular cells is mediated by endogenous transforming growth factor-beta. J Clin Invest. 1993; 92:1366–1372. [PubMed: 7690779]
70. Franch HA, Shay JW, Alpern RJ, et al. Involvement of pRB family in TGF beta-dependent epithelial cell hypertrophy. J Cell Biol. 1995; 129:245–254. [PubMed: 7698989]
71. Liu B, Preisig P. TGF-beta1-mediated hypertrophy involves inhibiting pRB phosphorylation by blocking activation of cyclin E kinase. Am J Physiol. 1999; 277:F186–194. [PubMed: 10444572]
72. Chen JK, Falck JR, Reddy KM, et al. Epoxyeicosatrienoic acids and their sulfonimide derivatives stimulate tyrosine phosphorylation and induce mitogenesis in renal epithelial cells. J Biol Chem. 1998; 273:29254–29261. [PubMed: 9786938]
73. Rao J, Otto WR. Fluorimetric DNA assay for cell growth estimation. Anal Biochem. 1992; 207:186–192. [PubMed: 1489093]

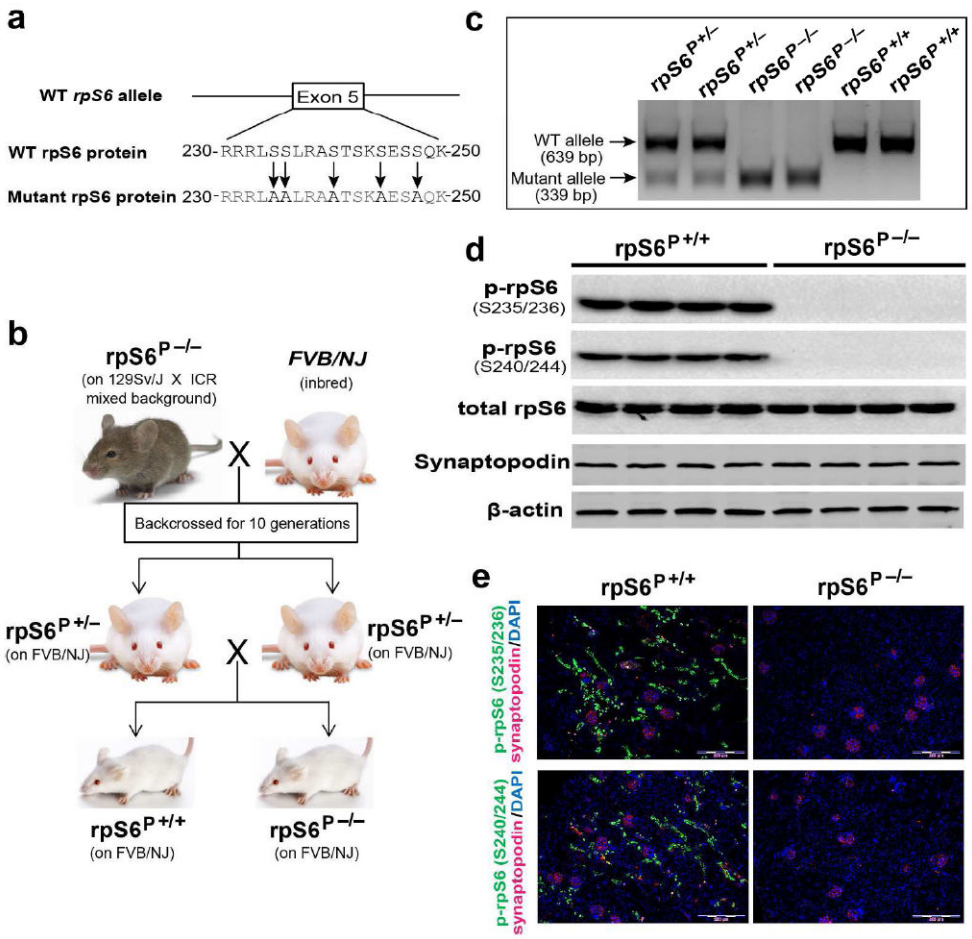


**Figure 1. Generation of congenic rpS6$^{P-/-}$ knock-in mice**

(**a**) Strategy for making rpS6$^{P-/-}$ knockin mice expressing unphosphorylatable 40S ribosomal protein rpS6, in which all five phosphorylatable serines (S235, S236, S240, S244, and S247) were replaced with alanines by site-directed mutagenesis. (**b**) A schematic depicting the generation of congenic rpS6$^{P-/-}$ knockin mice on FVB/NJ background.[28] Briefly, rpS6$^{P-/-}$ mice initially made on129Sv/J x ICR mixed genetic background were back-crossed onto the inbred FVB/NJ strain for 10 generations before intercrossing the resultant heterozygous offsprint (rpS6$^{P+/-}$) to produce homozygous congenic rpS6$^{P-/-}$ mice and rpS6$^{P+/+}$ littermates, used as control. (**c**) PCR genotyping detected only the 339-bp mutant allele in homozygous knockin mice (rpS6$^{P-/-}$), detected only the 639-bp wild type allele in their wild type littermates (rpS6$^{P+/+}$) but detected both the 339-bp and 639-bp bands in the heterozygous mice (rpS6$^{P+/-}$). (**d**) Immunoblotting and (**e**) Immunofluorescence staining with the indicated antibodies confirmed complete deletion of S6 phosphorylation in the kidney sections. Equal loading was confirmed by immunoblotting with a β-actin antibody (**d**). Synaptopodin, a marker for podocytes, was used for co-immunofluorescence staining to visualize the locations of glomeruli relative to phospho-rpS6-positive renal tubules (**e**). Shown are representative blots and images from one of three separate experiments with similar results.

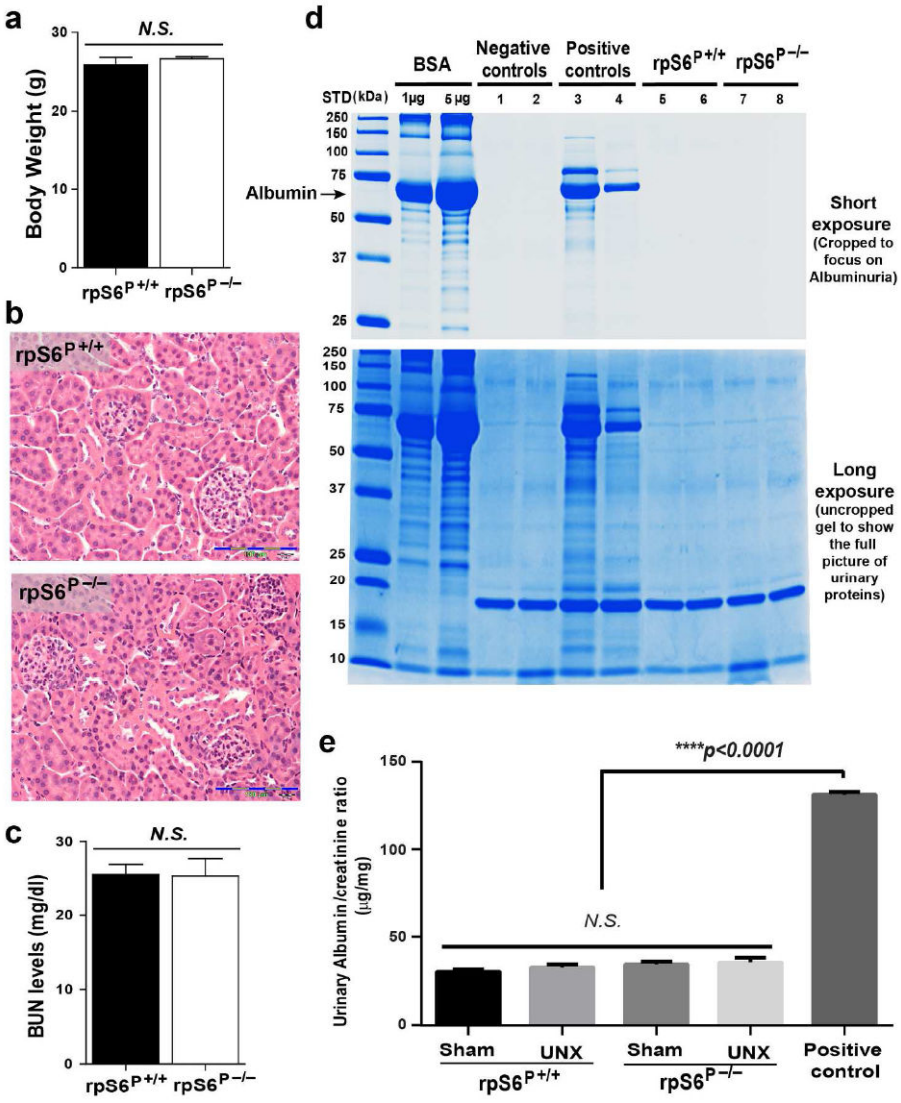


**Figure 2. Deletion of rpS6 phosphorylation had no effect on the body weight, renal histology, and kidney function**

8-week-old rpS6$^{P-/-}$ mice were used for comparison with their rpS6$^{P+/+}$ littermates. (**a**) rpS6$^{P-/-}$ mice had a mean body weight similar to that of their rpS6$^{P+/+}$ littermates. (**b**) H&E staining showed comparable renal histology in rpS6$^{P-/-}$ and rpS6$^{P+/+}$ littermates. (**c**) Both rpS6$^{P-/-}$ mice and their rpS6$^{P+/+}$ littermate had normal blood urea nitrogen (BUN) levels. (**d**) SDS-PAGE assay of the urine samples showed no proteinuria in rpS6$^{P-/-}$ and rpS6$^{P+/+}$ mice, although it clearly visualized proteinuria in 2~3-week-old podocyte-specific mVps34 knockout mice, used as a positive control[32]. 1 and 5 μg bovine serum albumin (BSA) were used as additional controls to show the location of albumin if there were any albuminuria (upper panel). Even after a long time exposure of the same gel (lower panel, uncropped gel showing the full spectrum of urinary protein profiles), there were only minimal amounts of different proteins in the urines of rpS6$^{P-/-}$as well as their rpS6$^{P+/+}$ littermates that were indistinquishable from those seen in the urines of mVps34 wild type mice (negative controls). Note that one protein at the size of 1~8 KD appeared to be the most abundant

urinary protein but it existed with equivalent abundance in the urined of all mice examined (lower panel). Shown are representative images and a gel from one of three separate experiments with similar results. (**e**) No difference in urinary albumin/creatinine ratio (ACR) between $rpS6^{P-/-}$ and $rpS6^{P+/+}$ mice subjected to either UNX or sham operation, although the urinary ACR of podocyte-specific mVps34 knockout mice at 2-3 weeks of age, used as a positive control,[32] was significantly increased.

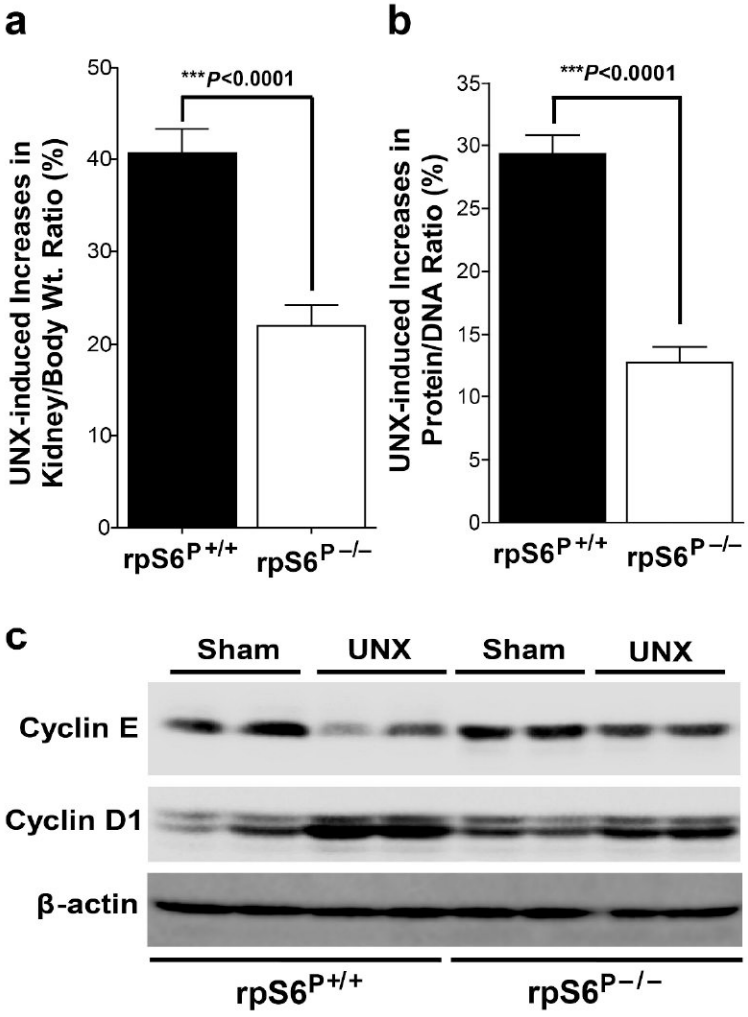


**Figure 3. Deletion of rpS6 phosphorylation inhibited cyclin D1 increase, cyclin E1 decrease, and compensatory renal hypertrophy induced by UNX**

rpS6$^{P-/-}$ and rpS6$^{P+/+}$ littermates at 8 weeks of age were subjected to right UNX or Sham surgery. UNX-induced renal hypertrophy 7 days after surgery was assessed by increases in left kidney/body weight ratio (**a**) and increases in protein/DNA ratio in the kidney (**b**), normalized by their sham-operated mice, respectively. Values are means ± SE ($n$ = 6-8) for each group. ***$P$ < 0.0001 indicates comparisons between rpS6$^{P+/+}$ mice ant rpS6$^{P-/-}$ littermates. Homogenates of left kidneys were subjected to immunoblotting with the antibodies specifically recognizing cyclin E1 and cyclin D1, respectively (**c**). Shown is a representative blot from one of three separate experiments with similar results.

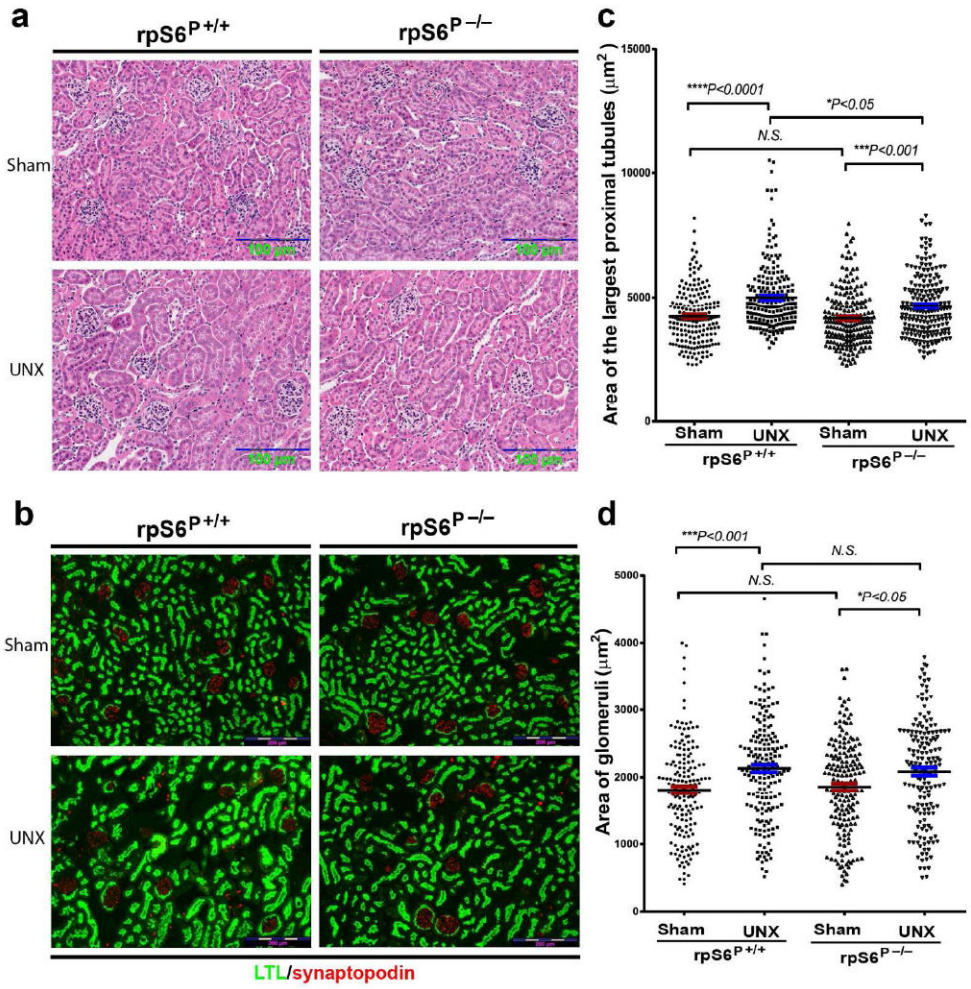


**Figure 4. Deletion of rpS6 phosphorylation inhibited the enlargement of proximal tubules but not the enlargement of glomeruli induced by UNX**

rpS6$^{P-/-}$ and rpS6$^{P+/+}$ littermates at 8 weeks of age were subjected to right UNX or Sham surgery. 7 days after surgery, UNX-induced histological changes in the left kidney were assessed by H&E staining (**a**) and double immunofluorescence staining (**b**). The area of proximal tubules (**c**) and the area of glomeruli (**d**) were measured as detailed in the *Methods*. Values are means ± SE (all glomeruli and 10 largest proximal tubules from 5 images per kidney section so 250 largest proximal tubules from *n* of 5 mice per group were measured for comparison).

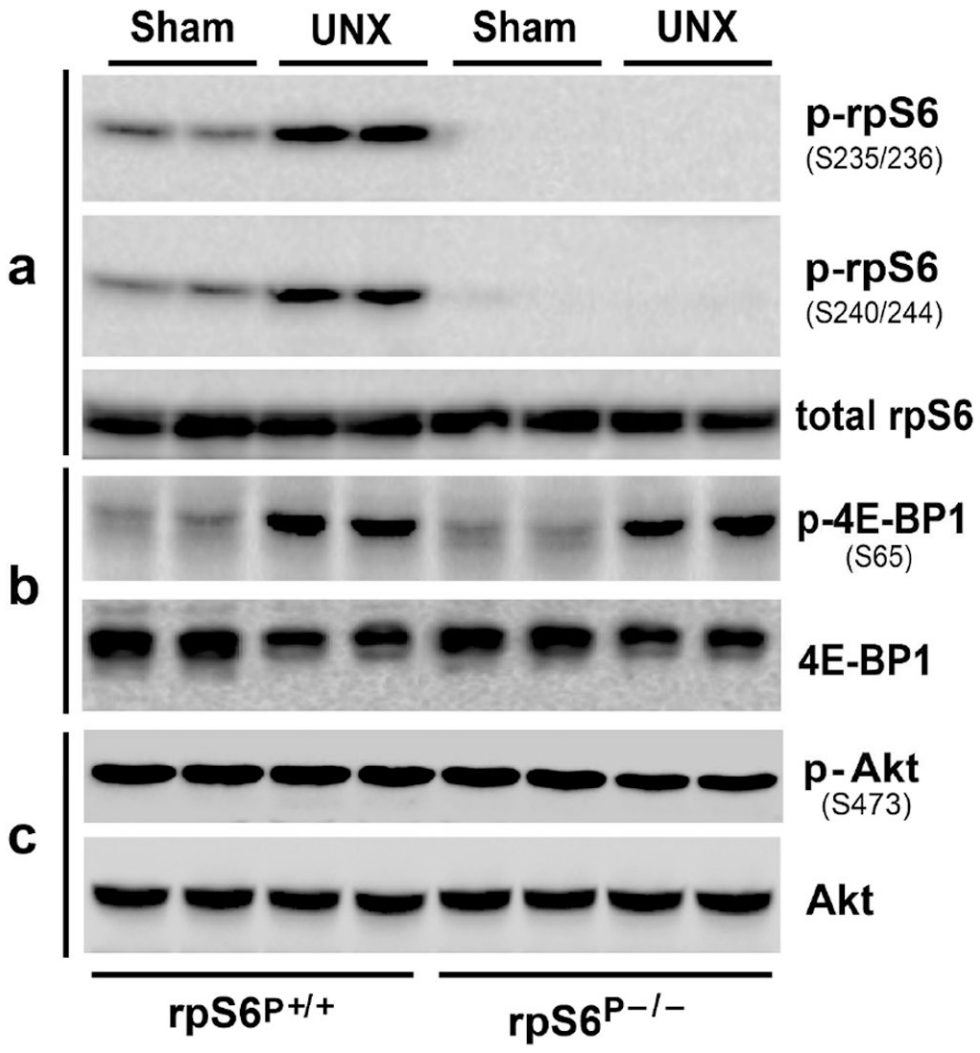


**Figure 5. Deletion of rpS6 phosphorylation had no effect on mTORC1 activation in the remaining kidney in response to UNX**

$rpS6^{P-/-}$ and $rpS6^{P+/+}$ littermates at 8 weeks of age were subjected to right UNX or Sham surgery. The mice were euthanized 7 days after the surgery, and left kidney homogenates were subjected to immunoblotting analysis with the indicated antibodies. All of the blots shown are representative blots of 3 separate experiments with similar results.

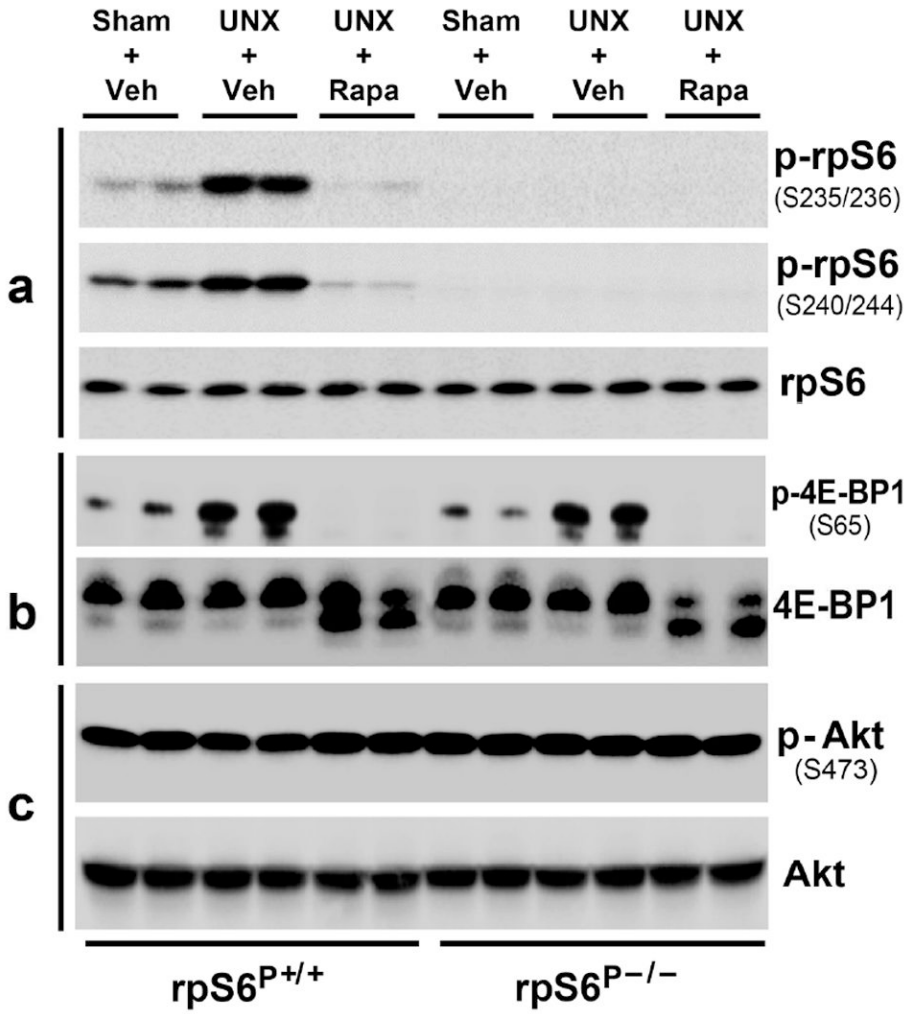


**Figure 6. Rapamycin inhibited phosphorylation of both 4E-BP1 and rpS6 but had no effect on the phosphorylation of Akt**

Eight-week-old rpS6$^{P-/-}$ mice and their rpS6$^{P+/+}$ littermates were pretreated with rapamycin (1 mg/kg body wt. intraperitoneally) or vehicle alone 2 h before right UNX or Sham surgery, followed by administration of rapamycin or vehicle once every two days. Seven days after the surgery, the mice were euthanized, and left kidney homogenates were subjected to immunoblotting analysis with the indicated antibodies. Shown are representative blots from one of three separate experiments with similar results.

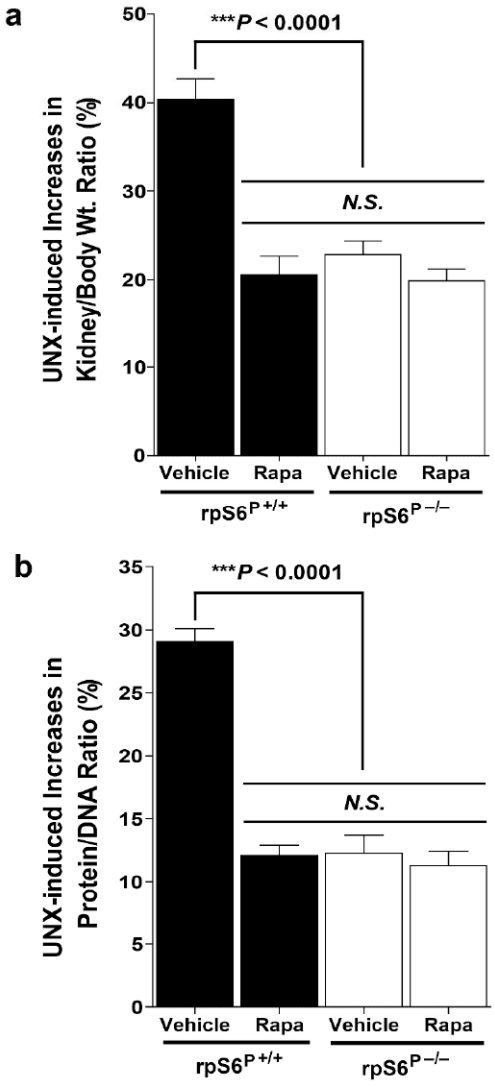


**Figure 7. Inhibition of rapamycin on UNX-induced compensatory renal hypertrophy in rpS6$^{P+/+}$ mice but not in rpS6$^{P-/-}$ knockin littermates**

Eight-week-old rpS6$^{P-/-}$ mice and their rpS6$^{P+/+}$ littermates were pretreated with rapamycin (1 mg/kg body wt. by intraperitoneal injection) or vehicle alone for 2 h before right UNX or Sham surgery, followed by administration of rapamycin or vehicle once every two days. The mice were euthanized 7 days after the surgery, UNX-induced compensatory renal hypertrophy was assessed by increases in kidney/body weight ratios (**a**) as well as increases in protein/DNA ratios (**b**). Values are means ± SE ($n$ = 5-6 for each group); ***$P$ < 0.0001 indicates comparisons between vehicle-treated rpS6$^{P+/+}$ mice and rapamycin-treated rpS6$^{P+/+}$ mice as well as vehicle- or rapamycin-treated rpS6$^{P-/-}$ littermates. The increases in kidney/body weight ratios and protein/DNA ratios did not show significant statistical difference among rapamycin-treated rpS6$^{P+/+}$ mice, vehicle-treated rpS6$^{P-/-}$ mice, and rapamycin-treated rpSe$^{-/-}$ mice.

## Table 1

Body weight, left kidney weight, and left kidney/body weight ratio in rpS6$^{P+/+}$ and rpS6$^{P-/-}$ mice 7 days after Sham or UNX surgery.

| Mouse Genotype/Surgery | Body weight, g | Left kidney weight, g | Left kidney/Body Wt. Ratio, % |
|---|---|---|---|
| S6$^{p+/+}$/Sham | 26.43 ± 0.56 | 0.185 ± 0.006 | 0.701 ± 0.024 |
| S6 $^{p+/+}$/UNX | 26.10 ± 0.71 | 0.258 ± 0.005 [a] | 0.987 ± 0.018 [c] |
| S6$^{p-/-}$/Sham | 27.11 ± 0.40 | 0.181 ± 0.003 | 0.668 ± 0.010 |
| S6$^{p-/-}$/UNX | 26.95 ± 0.57 | 0.220 ± 0.004 [b] | 0.815 ± 0.015 [d] |

Values are expressed as means ± SE ($n$ = 6-8 for each group). There was no statistical difference in the body weight among the 4 experimental groups.

[a] $P < 0.0001$ rpS6$^{P+/+}$/UNX vs. rpS6$^{P+/+}$/Sham;

[b] $P < 0.0001$ rpS6$^{P-/-}$/UNX vs. rpS6$^{P-/-}$/Sham and rpS6$^{P-/-}$/UNX vs. rpS6$^{P+/+}$/UNX;

[c] $P < 0.0001$ rpS6$^{P+/+}$/UNX vs. rpS6$^{P+/+}$/Sham;

[d] $P < 0.0001$ rpS6$^{P-/-}$/UNX vs. rpS6$^{P-/-}$/Sham and rpS6$^{P-/-}$/UNX vs. rpS6$^{P+/+}$/UNX.

## Table 2

Rapamycin inhibited UNX-induced compensatory renal hypertrophy in rpS6$^{P+/+}$ mice but not in rpS6$^{P-/-}$ knockin mice.

| Mouse Genotype/Surgery | Body weight, g | Left kidney weight, g | Left kidney/Body Wt. Ratio, % |
|---|---|---|---|
| rpS6$^{p+/+}$/Sham/Veh | 26.84 ± 0.38 | 0.184 ± 0.005 | 0.686 ± 0.018 |
| rpS6$^{p+/+}$/UNX/Veh | 26.60 ± 0.53 | 0.253 ± 0.004 *a* | 0.957 ± 0.016 *d* |
| rpS6$^{p+/+}$/UNX/Rapa | 26.76 ± 0.58 | 0.221 ± 0.004 *b* | 0.827 ± 0.014 *e* |
| rpS6$^{p-/-}$/Sham/Veh | 27.15 ± 0.39 | 0.181 ± 0.006 | 0.665 ± 0.007 |
| rpS6$^{p-/-}$/UNX/Veh | 26.90 ± 0.38 | 0.220 ± 0.003 *c* | 0.817 ± 0.010 *f* |
| rpS6$^{p-/-}$/UNX/Rapa | 26.74 ± 0.44 | 0.213 ± 0.002 | 0.797 ± 0.009 |

Values are expressed as means ± SE (n = 5-12 for each group). There was no statistical difference in the body weight among the 6 experimental groups (P = N.S.).

*a* $P < 0.0001$ rpS6$^{P+/+}$/UNX/Veh vs. rpS6$^{P+/+}$/Sham/Veh;

*b* $P < 0.0001$ rpS6$^{P+/+}$/UNX/Rapa vs. rpS6$^{P+/+}$/UNX/Veh and rpS6$^{P+/+}$/UNX/Rapa vs. rpS6$^{P+/+}$/Sham/Veh;

*c* $P < 0.0001$ rpS6$^{P-/-}$/UNX/Veh vs. rpS6$^{P-/-}$Sham/Veh and rpS6$^{P-/-}$/UNX/Veh vs. rpS6$^{P+/+}$/UNX/Veh;

*d* $P < 0.0001$ rpS6$^{P+/+}$/UNX /Veh vs. rpS6$^{P+/+}$/Sham/Veh;

*e* $P < 0.0001$ rpS6$^{P+/+}$/UNX/Rapa vs. rpS6$^{P+/+}$/UNX/Veh and rpS6$^{P+/+}$/UNX/Rapa vs. rpS6$^{P+/+}$/Sham/Veh;

*f* $P < 0.0001$ rpS6$^{P-/-}$/UNX/Veh vs. vS6$^{P-/-}$/Sham/Ven and vS6$^{P-/-}$/UNX/Veh vs. rpS6$^{P+/+}$/UNX/Veh.